CONTENTS

1 SEARCH FOR TOP SQUARKS IN ALL-HADRONIC FINAL STATES

In God we trust. All others must bring data.

William E. Deming

In this chapter the core of this thesis will be presented, namely the search for the direct pair-production of the supersymmetric partner of the top quark in all-hadronic final states using pp collisions, at a centre-of-mass energy $\sqrt{s}$ = 13 TeV, delivered by the Large Hadron Collider (LHC) and collected by the A Toroidal LHC ApparatuS (ATLAS) detector. A dataset of 36.1 fb^{-1} was used. Such measured value of integrated luminosity has an uncertainty of 3.2% based on studies of scans of the $x-y$ beam separation carried out on both 2015 and 2016 datasets, where the average pileup parameter μ was 13.7 and 24.9, respectively.

The results produced were published in a paper in the Journal of High Energy Physics in September 2017 [1]. A previous version of the analysis was also made public, using 13.3 fb^{-1} collected at $\sqrt{s}$ = 13 TeV, with an earlier subset of the whole 2015 + 2016 dataset, documented in an ATLAS conference note [2]. Although both versions contain author's contributions, only the results of the most recent analysis will be hereby discussed, as it represents the most updated, improved and extended version. Specifically, the optimisation of the search strategy, as well as the data-driven estimation of the number of events in the search regions for one of the most important backgrounds, and the evaluation of the related theory uncertainties, characterised the author's contributions. In addition, exception made for the optimisation strategy, the same contributions were also used in a different Supersymmetry (SUSY) analysis published in October 2017 in [3]. Further details can be found in Appendix A.

The chapter will be structured as it follows: an excursus on the simplified SUSY models considered will be presented in Section 1.1; the selection of the events and the objects used in both data and Monte Carlo (MC) will be presented in Section 1.3; the variables used and the optimisation of the regions in which the SUSY signals were searched for will be presented in Section 1.4; the nominal procedure used for the background estimation will be discussed in Section **??**, with particular focus on the data-driven background estimation in Section **??**; the results, together with their interpretation, will finally be presented in Section **??**.

1.1 SUSY Signals

As already introduced in Section **??**, the signals considered in this work are generated using simplified models, meaning that only the $\tilde{t}$, the $\tilde{\chi}_1^0$, the $\tilde{\chi}_2^0$, and the $\tilde{\chi}_1^\pm$, were the SUSY particles considered. In particular, in such considered models, either $\tilde{\chi}_2^0$ or $\tilde{\chi}_1^\pm$ is assumed to be the Next Lightest Supersymmetric Particle (NLSP) and, the chargino-neutralino mass splitting $\Delta m(\tilde{\chi}_1^\pm, \tilde{\chi}_1^0)$ is assumed to be 1 GeV, in accordance with the naturalness argument. This implies that the $\tilde{\chi}_1^\pm$ will promptly decay to $W^* \tilde{\chi}_1^0$, with the W emitted as a virtual particle. The decay products of the so-created virtual W will therefore be low p_T objects which will not be reconstructed by the ATLAS detector.

1.1.1 Benchmark processes

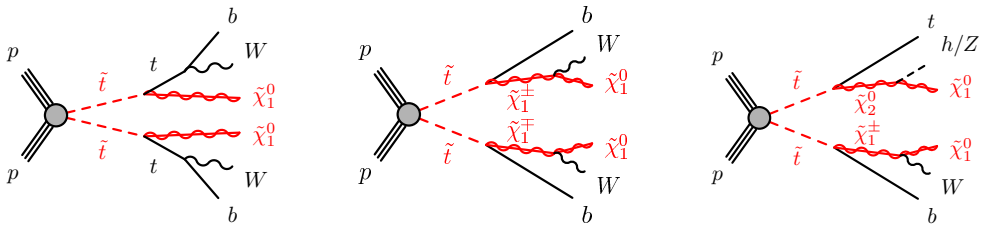

(a) $\tilde{t} \to t^{(*)} \tilde{\chi}_1^0$ (b) $\tilde{t} \to b\, \tilde{\chi}_1^\pm \to b W^{(*)} \tilde{\chi}_1^0$ (c) $\tilde{t} \to t\, \tilde{\chi}_2^0 \to h/Z\, \tilde{\chi}_1^0$

Figure 1.1: Diagrams of the decay topologies of the signal models considered in this work.

Figure 1.1(a)–(c) shows the diagrams corresponding to the decay scenarios considered in this work. In particular, (a) where both top squarks decay[1] via $\tilde{t} \to t^{(*)}\, \tilde{\chi}_1^0$; (b) where at least one of the stops decays via $\tilde{t} \to b\, \tilde{\chi}_1^\pm \to b\, W^{(*)}\, \tilde{\chi}_1^0$; (c) where $m_{\tilde{\chi}_2^0}$ is small enough to allow one stop to decay via $\tilde{t} \to t\, \tilde{\chi}_2^0 \to h/Z\, \tilde{\chi}_1^0$ where h is the Standard Model (SM) Higgs boson;

The results were interpreted in the simplified models where only one- and two-step decays scenarios are allowed and, as already mentioned, the latter will be referred to as a natural SUSY-inspired mixed grid, i. e. $\Delta m(\tilde{\chi}_1^\pm, \tilde{\chi}_1^0) = 1$ GeV [4, 5, 6]. Furthermore, in both scenarios the Lightest Supersymmetric Particle (LSP) is considered to be a pure bino state. The results will also be interpreted in two slices of the Phenomenological Minimal Supersymmetric Standard Model (MSSM) (pMSSM) models: wino-NLSP and well-tempered neutralino pMSSM [7, 8]. A fourth scenario, in addition to direct pair production, was considered: top squarks can also be indirectly produced via gluino decays, as illustrated in Figure 1.2. In such model, the mass difference

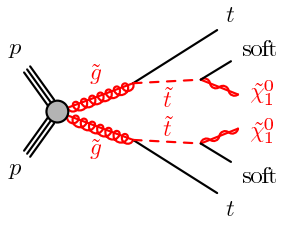

Figure 1.2: Diagram of the gluino-mediated top squark production. The term “soft" refers to decay products whose transverse momenta are below the detector thresholds.

[1] The symbol (*) indicates off-shell production

between the top squark and the neutralino is considered to be relatively small, $\Delta m(\tilde{t}_1, \tilde{\chi}_1^0) = 5$ GeV, allowing the jets originating from $\tilde{t}_1$ decay to have a p_{T} below the reconstruction threshold of the ATLAS detector resulting in an experimental signature nearly equivalent to the one in Figure 1.1(a).

1.1.2 MC samples

A grid of points across the $(m_{\tilde{t}_1} - m_{\tilde{\chi}_1^0})$ plane with a 50-GeV spacing is generated to simulate the above-mentioned simplified models. The signal models were generated using `MG5_aMC@NLO 2.2-2.4` [9] interfaced to `PYTHIA8` [10] for the Parton Shower (PS) and hadronisation. `EvtGen 1.2.0` [11] was employed for the decays of the b- and c-hadrons. The tree-level Matrix Element (ME) calculation includes the emission of up to two additional partons for all signal samples. The `NNPDF2.3LO` Parton Distribution Function (PDF) [12] set was used to generate the signal samples with the `A14` [13] tune for the Underlying Event (UE) and shower parameters. Additionally, the CKKW-L prescription [14] was used for the ME–PS matching.

The various signal cross sections were all calculated to next-to-leading order in the strong coupling constant, with the addition of soft-gluon emission re-summation at next-to-leading-logarithm accuracy (NLO+NLL) [15, 16, 17]. The sparticle mass spectra for pMSSM models were calculated using `Softsusy 3.7.3` [18, 19] while the decays of each sparticle were performed by `HDECAY 3.4` [20] and `SDECAY 1.5/1.5a` [21]. Finally, various PDF sets, factorisation, and re-normalisation scales were used to generate an envelope of cross-section predictions, within which a nominal value and uncertainty were chosen. Further details can be found in [22].

1.2 Objects definition

The physics objects, as output of the reconstruction algorithms discussed in Section **??**, are required to pass a first loose selection to be categorised as *baseline* objects. An additional procedure is employed, to remove potentially overlapping objects, e. g. a lepton is identified as a jet, or a lepton that falls within the same jet cone. The so-called Overlap Removal (OR) procedure, whose inputs are two baseline objects, is employed to resolve such ambiguity by discarding on of the two objects by looking at their ΔR as shown in Table 1.1.

The data-driven estimation of $t\bar{t}$+Z events using $t\bar{t}$+γ is the only part of the analysis that used reconstructed photons. In particular, the OR is modified accordingly to avoid that an object will appear in multiple collections (double-counting). The various baseline and signal objects can now be defined as it follows:

Electrons baseline electrons are required to have $|\eta| < 2.47$, $p_{\mathrm{T}} > 7$ GeV and have to pass a variant of the `VeryLoose` likelihood-based selection (further details in [23, 24]). Electron candidates which pass the OR, have a $p_{\mathrm{T}} > 20$ GeV ($p_{\mathrm{T}} > 28$ GeV) in regions with a $E_{\mathrm{T}}^{\mathrm{miss}}$ (lepton) trigger, satisfy $d_0/\sigma_{d_0} < 5$, $z_0 \sin\theta < 0.5$, and pass a `Tight` likelihood-based selection isolation, are tagged as signal;

Table 1.1: List of the possible ambiguities with relative criteria and decisions.

Ambiguity	Criterion	Object kept	Object removed
electron/jet	$\Delta R(e,\text{jet}) < 0.2$	electron	jet
	$0.2 \leq \Delta R(e,\text{jet}) < 0.4$	jet	electron
electron/b−jet	$\Delta R(e,b\text{−jet}) < 0.2$	b−jet	electron
muon/jet	$\Delta R(\mu,\text{jet}) < 0.4$ and $N_{\text{tracks}} < 3$, $p_{\text{T}}^{\text{track}} > 500$ MeV	muon	jet
photon/electron	$\Delta R(e,\gamma) < 0.4$	electron	photon
photon/muon	$\Delta R(\mu,\gamma) < 0.4$	muon	photon
photon/jet	$\Delta R(\text{jet},\gamma) < 0.4$	jet	photon

Muons baseline muons have to pass a `Loose` selection [25], satisfy $|\eta| < 2.7$ and $p_{\text{T}} > 6$ GeV. Further requirements are imposed on muon candidates to tag them as signal. In particular, they have to pass the OR, a `Medium` quality selection [25], and satisfy $|d_0| < 3\sigma_{d_0}$ and $|z_0 \times \sin\theta| < 0.5$. Additionally, the p_{T} requirement is tightened up to 20 GeV (28 GeV) in regions with a $E_{\text{T}}^{\text{miss}}$ (lepton) trigger;

Photons baseline photons have to pass a `Tight` [26] selection, and have $p_{\text{T}} > 25$ GeV and $|\eta| < 2.37$. Additionally, baseline photon candidates are required to have $p_{\text{T}} > 130$ GeV and satisfy a tighter isolation selection, in order to be tagged as signal;

Jets as already mentioned in Chapter **??**, jets are reconstructed using the anti-k_t algorithm with $R = 0.4$. Baseline jets are required to have $p_{\text{T}} > 20$ GeV and $|\eta| < 4.8$. Signal jets have to pass the OR, satisfy the Jet vertex Tagger (JVT) requirement, and have $|\eta| < 2.8$ and $p_{\text{T}} > 20$ GeV.

b-tagged jets baseline jets in the event are identified as originating from the decay of a b-quark is based on the `MV2c10` jet tagger which uses the a 77% fixed-cut WP. The p_{T} threshold applied to signal jets is also applied to b−jet and the requirement on the pseudorapidity is relaxed down to $|\eta| < 2.5$.

Missing transverse energy The $E_{\text{T}}^{\text{miss}}$ is reconstructed as described in Section **??**. Baseline muons, electrons, and jets after overlap removal are used in the $E_{\text{T}}^{\text{miss}}$ recalculation.

Additionally, in the analysis carried out during Run-1 [27] another $E_{\text{T}}^{\text{miss}}$-related quantity was introduced. The track-based $E_{\text{T}}^{\text{miss}}$, derived from the sum of the p_{T} of the tracks associated with the objects in the event was found to have discriminating power to reject fake $E_{\text{T}}^{\text{miss}}$. The $\mathbf{p}_{\text{T}}^{\text{miss,track}}$, whose magnitude is $E_{\text{T}}^{\text{miss,track}}$, from the tracking system is computed using the vector sum of the reconstructed inner detector tracks, $\mathbf{p}_{\text{T}}^{\text{miss,track}} = \sum_i^{\text{tracks}} p_{\text{T}}^i$, with $p_{\text{T}} > 500$ MeV and $|\eta| < 2.5$, that are associated with the Primary Vertex (PV) in the event.

Ultimately, leptons are also required to satisfy p_{T}-dependent track- and calorimeter-based isolation criteria. The calorimeter-based isolation is determined by taking the ratio of the sum

of energy deposits in a cone of $R = 0.2$ around the electron or muon candidate and the energy deposits associated with the electron and muon. The track-based isolation is estimated in a similar way but using a variable cone size with a maximum value of $R = 0.2$ for electrons and $R = 0.3$ for muons. An isolation requirement is made that is 95% efficient for electron or muon candidates with $p_{\mathrm{T}} = 25$ GeV and 99% for candidates with $p_{\mathrm{T}} = 60$ GeV.

1.3 Event Selection

The ATLAS detector did not operate with the same conditions during 2015 and 2016, meaning that different triggers and objects (calibration parameters) were used. In order for MC parameters to be modified consistently with what is done in data, MC events are assigned a random number, which identifies an ATLAS run. This allows MC events to be associated with specific data-taking periods such that their parameters are associated what is done in data and can be modified accordingly.

Triggers

As previously discussed at the end of Chapters **??** and in Chapter **??**, physics events are recorded once they passed a certain trigger. In particular, a $E_{\mathrm{T}}^{\mathrm{miss}}$ trigger is used to select events that fall in signal-enriched regions, Signal Region (SR), where 0 leptons (ℓ) are required; a single-lepton (photon) trigger is used for background-enriched regions, where 1-lepton (photon) is required. A breakdown of all the lowest unprescaled online triggers used will be presented below;

Missing transverse energy once the $E_{\mathrm{T}}^{\mathrm{miss}}$ is reconstructed from an input jet collection, a 70-GeV threshold is required in the 2015 dataset whereas, due to the increase in instantaneous luminosity (impact on the trigger rate), in 2016 the threshold was gradually raised to 90, 100, and 110 GeV. It can be seen (Figure **??**) that for analysis purposes a cut of at least 200 GeV is required to stay in a region where the trigger is fully efficient (*plateau*);

Single electron events with an electron are triggered on using a logic `OR` of three chains. In particular, the first consists of a 24-GeV (26-GeV) threshold, together with an Level-1 (L1) isolation, in 2015 (2016) data; the second chain uses a 60-GeV threshold without additional isolation requirement; the third uses a 120-GeV threshold to be efficient at high E_{T}; a $p_{\mathrm{T}}^{e} > 27$ GeV cut is applied to stay in the plateau region;

Single muon a logic `OR` of two chains is instead used to trigger events with muons; a first chain with a 20-GeV threshold is used in data 2015 and 26-GeV threshold, together with an isolation requirement, in 2016; a second chain with a 50-GeV threshold is employed for both 2015 and 2016 data; a $p_{\mathrm{T}}^{\mu} > 27$ GeV is applied to stay in the plateau region;

Single photon unlike the lepton case, only one chain is used to select events with photons; a 120 GeV (140 GeV) threshold is employed in 2015 (2016). Additionally, in order to ensure full trigger efficiency a $p_{\mathrm{T}}^{\gamma} > 150$ GeV cut is applied.

Event cleaning

In order to remove events where the a detector fault occurred, a set of offline cuts is applied. The first requirement for an event to be a good physics event, is the existence of a primary vertex with a minimum of two tracks, with $p_{\mathrm{T}} > 400$ MeV, associated with it. Once this is passed, the status of both Electromagnetic Calorimeter (ECAL) and Hadronic Calorimeter (HCAL) for that event is checked: if any of the calorimeters returned an error state, the event is discarded. In addition, to reduce and suppress the fake-jet contamination a *bad jet* requirement is defined by introducing quality requirements on a variety of jet parameters, e. g. the fraction of energy deposited in the different layers of the calorimeters, and the fraction of jet p_{T} measured by the tracks in the Inner Detector. Events containing bad jets that passed the OR are discarded. Similarly, events containing baseline muon candidates, whose relative uncertainty on e/p is larger than 20%, and which were found before the OR, are discarded. This also applies to events containing those potentially cosmic muons which were not removed by the OR.

1.4 Signal Regions

$t\bar{t}$+Z ESTIMATION IN DM PLUS HEAVY FLAVOUR

The data-driven background estimation technique and the theory uncertainties calculation prescription already discussed in Chapter 1 were also employed in the search for dark matter produced in association with third-generation quarks, which was published in October 2017 in the Eur. Phys. J. [3]. This analysis also used 36.1 fb^{-1} of pp collisions delivered by the LHC and recorded with the ATLAS detector, and although it targeted various final states with different number of leptons, depending on the $t\bar{t}$ decay modes, the author's contribution was only used for the experimental signature shown in Figure A.1, as this is identical to the final states discussed in Chapter 1, namely the one shown in Figure 1.1: 4 or more jets plus missing transverse momentum.

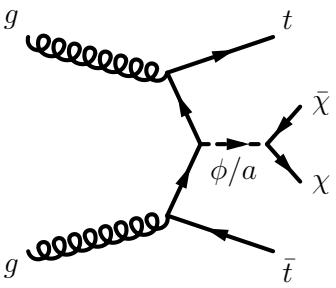

Figure A.1: Representative diagrams at the lowest order for spin-0 mediator associated production with top quarks $t\bar{t}$ + ϕ/a (taken from [3])

The objects used, and the variables employed in the design of a region of control for the $t\bar{t}$+γ process, are the same as those used in the analysis already discussed in Chapter 1. Only one set of 2 SR was used. Table bla shows the selection of the two SRs.

Table bla shows the control region selection employed (CRγ) to isolate the $t\bar{t}$+γ process. This essentially is identical to Table blabla already shown in Chapter 1. A purity of bla% was reached and a scale factor of 1.whatever was obtained.

Figure bla2 shows the distribution of the $E_{\mathrm{T}}^{\mathrm{miss}}$ in CRγ where a very good data/MC agreement was found.

The procedure adopted to estimate the contribution of the theory uncertainties to the total uncertainty is also the same and the results are shown in Table bla, where the highest uncertainty of whatever% was obtained for SR bla.

LIST OF ACRONYMS

ATLAS A Toroidal LHC ApparatuS

ECAL Electromagnetic Calorimeter

HCAL Hadronic Calorimeter

JVT Jet vertex Tagger

L1 Level-1

LHC Large Hadron Collider

LSP Lightest Supersymmetric Particle

MC Monte Carlo

ME Matrix Element

MSSM Minimal Supersymmetric Standard Model

NLSP Next Lightest Supersymmetric Particle

OR Overlap Removal

PDF Parton Distribution Function

pMSSM Phenomenological MSSM

PS Parton Shower

PV Primary Vertex

SM Standard Model

SR Signal Region

SUSY Supersymmetry

UE Underlying Event

BIBLIOGRAPHY

[1] ATLAS Collaboration, M. Aaboud et al., *Search for a scalar partner of the top quark in the jets plus missing transverse momentum final state at $\sqrt{s}$=13 TeV with the ATLAS detector*, JHEP **12** (2017) 085, arXiv:1709.04183 [hep-ex]. 1

[2] ATLAS Collaboration, M. Aaboud et al., *Search for the Supersymmetric Partner of the Top Quark in the Jets+$E_{\mathrm{T}}^{\mathrm{miss}}$ Final State at $\sqrt{s}$ = 13 TeV,*. 1

[3] ATLAS Collaboration, M. Aaboud et al., *Search for dark matter produced in association with bottom or top quarks in $\sqrt{s}$ = 13 TeV pp collisions with the ATLAS detector*, arXiv:1710.11412 [hep-ex]. 1, 7

[4] J. Alwall, M.-P. Le, M. Lisanti, and J. G. Wacker, *Searching for directly decaying gluinos at the Tevatron*, Phys. Lett. B **666** (2008) 34–37, arXiv:0803.0019 [hep-ph]. 2

[5] J. Alwall, P. Schuster, and N. Toro, *Simplified models for a first characterization of new physics at the LHC*, Phys. Rev. D **79** (2009) 075020, arXiv:0810.3921 [hep-ph]. 2

[6] LHC New Physics Working Group Collaboration, D. Alves, *Simplified models for LHC new physics searches*, J. Phys. G **39** (2012) 105005, arXiv:1105.2838 [hep-ph]. 2

[7] A. Djouadi et al., *The Minimal supersymmetric standard model: Group summary report*, arXiv:9901246 [hep-ph]. 2

[8] C. F. Berger, J. S. Gainer, J. L. Hewett, and T. G. Rizzo, *Supersymmetry without prejudice*, JHEP **02** (2009) 023, arXiv:0812.0980 [hep-ph]. 2

[9] J. Alwall, R. Frederix, S. Frixione, V. Hirschi, F. Maltoni, O. Mattelaer, H. S. Shao, T. Stelzer, P. Torrielli, and M. Zaro, *The automated computation of tree-level and next-to-leading order differential cross sections, and their matching to parton shower simulations*, JHEP **07** (2014) 079, arXiv:1405.0301 [hep-ph]. 3

[10] T. Sjöstrand, S. Mrenna, and P. Z. Skands, *A brief introduction to PYTHIA 8.1*, Comput. Phys. Commun. **178** (2008) 852–867, arXiv:0710.3820 [hep-ph]. 3

[11] D. J. Lange, *The EvtGen particle decay simulation package*, Nucl. Instrum. Meth. **462** no. 1–2, (2001) 152 – 155. 3

[12] R. D. Ball et al., *Parton distributions with LHC data*, Nucl. Phys. B **867** (2013) 244–289, arXiv:1207.1303 [hep-ph]. 3

[13] H.-L. Lai, M. Guzzi, J. Huston, Z. Li, P. M. Nadolsky, J. Pumplin, and C. P. Yuan, *New parton distributions for collider physics*, Phys. Rev. D **82** (2010) 074024, arXiv:1007.2241 [hep-ph]. 3

[14] L. Lönnblad and S. Prestel, *Merging multi-leg NLO matrix elements with parton showers*, JHEP **03** (2013) 166, arXiv:1211.7278 [hep-ph]. 3

[15] W. Beenakker, M. Kramer, T. Plehn, M. Spira, and P. M. Zerwas, *Stop production at hadron colliders*, Nucl. Phys. **B515** (1998) 3–14, hep-ph/9710451. 3

[16] W. Beenakker, S. Brensing, M. Kramer, A. Kulesza, E. Laenen, and I. Niessen, *Supersymmetric top and bottom squark production at hadron colliders*, JHEP. **1008** (2010) 098, arXiv:1006.4771 [hep-ph]. 3

[17] W. Beenakker, S. Brensing, M. Kramer, A. Kulesza, E. Laenen, et al., *Squark and gluino hadroproduction*, Int.J.Mod.Phys. **A26** (2011) 2637–2664, arXiv:1105.1110 [hep-ph]. 3

[18] B. Allanach, *SOFTSUSY: a program for calculating supersymmetric spectra*, Comput. Phys. Commun. **143** (2002) 305–331, arXiv:hep-ph/0104145. 3

[19] B. Allanach, P. Athron, L. C. Tunstall, A. Voigt, and A. Williams, *Next-to-minimal SOFTSUSY*, Comput. Phys. Commun. **185** (2014) 2322–2339, arXiv:1311.7659 [hep-ph]. 3

[20] A. Djouadi, J. Kalinowski and M. Spira, *HDECAY: A Program for Higgs boson decays in the standard model and its supersymmetric extension*, Comput. Phys. Commun. **108** (1998) 56, arXiv:9704448 [hep-ph]. 3

[21] A. Djouadi, M. Muhlleitner and M. Spira, *Decays of supersymmetric particles: The Program SUSY-HIT (SUspect-SdecaY-Hdecay-InTerface)*, Acta. Phys. Polon. B **38** (2007) 635–644, arXiv:0609292 [hep-ph]. 3

[22] C. Borschensky, M. Kramer, A. Kulesza, M. Mangano, S. Padhi, T. Plehn, and X. Portell, *Squark and gluino production cross sections in pp collisions at $\sqrt{s}$ = 13, 14, 33 and 100 TeV*, Eur. Phys. J. C **74** (2014) 3174, arXiv:1407.5066 [hep-ph]. 3

[23] ATLAS Collaboration, ATLAS Collaboration, *Electron efficiency measurements with the ATLAS detector using 2012 LHC proton–proton collision data*, Eur. Phys. J. C **77** no. 3, (2017) 195, arXiv:1612.01456 [hep-ex]. 3

[24] ATLAS Collaboration, *Electron identification measurements in ATLAS using $\sqrt{s}$ = 13 TeV data with 50 ns bunch spacing*,. https://cds.cern.ch/record/2048202. 3

[25] ATLAS Collaboration, ATLAS Collaboration, *Muon reconstruction performance of the ATLAS detector in proton–proton collision data at $\sqrt{s}$ =13 TeV*, Eur. Phys. J. C **76** no. 5, (2016) 292, arXiv:1603.05598 [hep-ex]. 4

[26] ATLAS Collaboration, M. Aaboud et al., *Measurement of the photon identification efficiencies with the ATLAS detector using LHC Run-1 data*, Eur. Phys. J. **C76** no. 12, (2016) 666, arXiv:1606.01813 [hep-ex]. 4

[27] ATLAS Collaboration, *Search for direct pair production of the top squark in all-hadronic final states in proton-proton collisions at $\sqrt{s}$ = 8 TeV with the ATLAS detector*, JHEP **09** (2014) 015, arXiv:1406.1122 [hep-ex]. 4

This thesis was typeset using the LaTeX typesetting system created by Leslie Lamport.
The body text size is set to 11 pt with *Utopia Regular* with *Fourier* font, part of TeX Live.
The bibliography was typeset using the ATLAS-paper style.